Applied Physics A (2021) 127:37
https://doi.org/10.1007/s00339-020-04188-9

Applied Physics A
Materials Science & Processing

Synthesis of nanostructured hardystonite (HT) bioceramic coated on titanium alloy (Ti-6Al-4V) substrate and assessment of its corrosion behavior, bioactivity and cytotoxicity

Rasoul Asgarian[1] · Ahmad Khalghi[2] · Razieh Kiani Harchegani[3] · Marjan Monshi[1] · Delara Aarabi Samani[4] · Ali Doostmohammadi[4,5]

Received: 20 June 2020 / Accepted: 3 December 2020 / Published online: 3 January 2021
© The Author(s), under exclusive licence to Springer-Verlag GmbH, DE part of Springer Nature 2021

Abstract
Bioceramic coatings have had a significant impact on the realm of biomaterials and medical devices in recent decades. In this study, synthesized hardystonite coating ($Ca_2ZnSi_2O_7$) by sol–gel method was applied on titanium substrate (Ti-6Al-4V) using electrophoretic deposition method. XRD patterns and EDX result confirm the pure hardystonite phase structure. Transmission electron microscopy was confirmed the appeared round morphology and nanometer size of the synthesized hardystonite particles. Additionally SEM analysis was approved that the hardystonite coating is able to make a uniform and flawless apatite with needle-like and cauliflower forms during prolonged exposure to SBF. The Ringer's solution Tafel test results were indicated that the corrosion resistance of twice-coated samples is increased by increasing the voltage to 50 Voltages so that the corrosion current density in the twice coated samples is less than the bare samples. In vitro evaluation by MTT assay was confirmed the viability of the bone marrow stem cells so that hardystonite increases the vitality and reproduction of stem cells at low concentration which makes the hardystonite coating a suitable candidate for clinical applications.

Keywords Bioceramics · Hardystonite ($Ca_2ZnSi_2O_7$) · Ti-6Al-4V · Electrophoretic deposition (EPD) · Corrosion behavior · Cytotoxicity

1 Introduction

Bioceramics are the ceramics used for repair and reconstruction of diseased or damaged parts of the musculo-skeletal system [1]. Bioceramics may be bioinert (e.g., alumina and zirconia), resorbable (e.g., tricalcium phosphate), bioactive (e.g., hydroxyapatite, bioactive glasses, and glass–ceramics), or porous for tissue ingrowth (e.g., hydroxyapatite-coated metals) [2]. Bioceramics clinical applications are often associated with the skeleton system, bones, teeth, joints and extension, renovating and growth of soft and hard tissues of the body [3–8]. Clinical success requires the simultaneous achievement of a stable interface with connective tissue and a match of the mechanical behavior of the implant with the tissue to be replaced [2]. Since the mechanical properties of bioceramics are limited, they should not be overloaded and they can only tolerate the compressive loading [9–11]. In contrast, if an implant is loaded such that interfacial movement can occur, the implant loosens quickly. Loosening invariably leads to clinical failure, for a variety of reasons, including fracture of the implant or the bone adjacent to the implant [2].

Porous bioceramics can increase the interfacial area between the implant and the tissue results in an increased resistance to movement of the device in the tissue. The interface is established by the living tissue in the pores. However,

✉ Ali Doostmohammadi
Doost@yorku.ca

1 Advanced Materials Research Center, Faculty of Materials Engineering, Islamic Azad University, Najafabad Branch, Isfahan, Iran

2 Master of Materials Science and Engineering, Iran University of Science and Engineering (IUST), Tehran, Iran

3 Department of Mechanical, Automotive and Materials Engineering, University of Windsor, Windsor, ON N9B 3P4, Canada

4 Materials Department, Engineering Faculty, Shahrekord University, Shahrekord, Iran

5 Department of Mechanical Engineering, Lassonde School of Engineering, York University, 4700 Keele Street, Toronto, ON M3J 1P3, Canada

the limitation associated with porous implants is that, for the tissue to remain viable and healthy, pores must be > 100 to 150 μm in diameter to provide a blood supply to the host tissues [12]. When the material is a metal, the large increase in surface area can provide a focus for corrosion of the implant and loss of metal ions into the tissues, which can cause a variety of medical problems including sarcoma—a cancer that arises from transformed cells of connective tissue origin [13]. These potential problems can be diminished by using a bioactive ceramic material, such as hydroxyapatite (HA), as a coating on the porous metal [11, 14]. The property of such coating in transplanting with bones helps to installation and stabilization of orthopedics prosthesis and dental implants [15].

Several conventional techniques have been used to create coatings on metallic implants, such as thermal spraying, dynamic mixing, dip coating, sol–gel coating, electrostatic or electrophoretic deposition, biomimetic coating and hot isostatic pressing (HIP). Every technique has its own advantages and disadvantages. For example, the adhesion (bond strength) and the composition or thickness of the coating material are affected by the coating method employed. A comparative list of the pros and cons of the different traditional deposition methods used for implant coating is given in Table 1 [16]. Recently another methods based on laser technology, including pulsed laser deposition, laser cladding and matrix-assisted pulsed laser evaporation have gained a tremendous popularity in the medical industry [17].

Hydroxyapatite (HA) is a porous bioactive bioceramics that has reached a significant level of clinical application as a coating on the porous metal surface [2]. Among all of the bioactive materials, the most proper biocompatibility behavior belongs to HA bioceramics and bioglasses considered as a group of calcium phosphate compounds that attach to graft tissue in a short time [18]. But, its mechanical strength is inadequate and it is too brittle and fracture frequently. Its unique biological properties caused to be considered for the development of its properties rather than to be replaced with other materials. Calcium silicates such as $CaSiO_3$ and Ca_2SiO_4 among conventional ceramic materials can release calcium and silicate ions approved to influence the bone replacement and bone repair in the natural environment (in vivo) and out of natural environment (in vitro) [18]. Ceramic composites containing zinc are providing new opportunities in bone tissue engineering studies. Zinc deficiency makes slow growth of bones and some common defects in soft and hard tissues of humans and animals. Studies have shown that zinc plays a very important physiological role in the growth and bone mineralization. By aging, the amount of zinc gradually diminishes and bone density decreases. Studies proved that bio-materials containing zinc can provoke the activity of bone making cells and facilitate creating new bones [18–20]. Hardystonite (HT) ($Ca_2ZnSi_2O_7$) is a silicate ceramic compound containing zinc [7]; therefore, it seems to have appropriate function and properties to repair the hard tissues of the body. Wu et al. [7] added zinc to calcium silicate and synthesized the HT that owned higher mechanical properties (bending strength of 136.4 MPa and fracture toughness of 1.24 MPa $\sqrt{m}$ than HA. The bending strength of HAp has been reported to vary between 80 and 89.07 MPa and the fracture toughness between 0.75 and 1.0 MPa $\sqrt{m}$.

Hardystonite is currently recognized as a biocompatible bioceramic material for a range of medical applications.

Table 1 Comparison between different methods used for coating of implants [16]

Deposition method	Advantages	Disadvantages
Sol–gel method	Coats 3D complex porous substrates Low processing temperatures Relatively cheap Very thin coatings (< 1 μm)	Should be processed in a controlled atmosphere
Electrostatic deposition	Uniform coating thickness on flat substrates Relatively cheap	Only coats exposed area Coatings are fragile
Electrophoretic deposition	High deposition rates Uniform thickness of coating Coats complex 3D porous substrates	Cracks in coating High sintering temperatures
Thermal spraying	High deposition rates	Only coats exposed area Coating decomposition due to high temperature Rapid cooling may result in amorphous coating
Dip coating	Inexpensive Coatings applied quickly Coats complex 3D porous substrates	High sintering temperatures Film thickness can vary from top to bottom (wedge effect) Fragile coating due to high thickness (in mm range)
Hot isostatic pressing	Dense coatings	Unable to coat complex 3D porous substrates Expensive Requires high temperature

Although the excellent corrosion properties of Ti alloys have been proved, electrochemical researches on Ti (alloys)-HT composites are few. Moreover, very little literatures could be found regarding the relationship among structure, morphology and electrochemical characteristics when Ti alloy is composited with HT bioceramic coating.

Hardystonite is more chemically stable compared to calcium silicate (CS) ceramics like Ca_2SiO_4 and $CaMgSi_2O_6$, and the presence of Zn ions affects the roughness of the ceramic. In addition, 0.4 ppm Zn ions (50%Zn concentration) possesses the best chemical stability, contributes to HOB cell proliferation and differentiation and inhibits apatite formation [21]. Bagherpour et al. [19] stated that chemical stability of hardystonite was higher than calcium silicate ceramics as the presence of zinc ions that affected on the ceramic hardness. They also studied the corrosion behavior of hardystonite powder coated on stainless steel samples by electrophoretic method. They concluded that the potential of the coated samples and also polarization resistance of the coated samples (resistance of the system to corrosion) depends on the applied voltage and time during coating process. Their results show that the polarization rate of the coated samples in the optimum condition is 9 times better than bare stainless steel samples. Wang et al. revealed that the hardystonite-CS scaffold has a lower degradation rate compared to CS ceramics and hardystonite-CS scaffolds show better HOB attachment than CS scaffolds. Li et al. reported that with a hardystonite coating on Ti-6Al-4V alloy, chemical stability improves considerably [21].

The electrophoretic deposition (EPD) is one of the colloidal processes in ceramics generating and coating [7, 22]. The advantages of using such a process include short coating time, feasibility, as well as not having a restriction in the morphology of the substrate. In comparison with other coating methods, the EPD is more advanced, has more varieties, and it is easy to handle. For these reasons, it has achieved great acceptance of the researchers [22].

Electrophoretic deposition (EPD) process is based on the movement and deposition of charged particles under electric field onto a conductive electrode to develop thin or thick films and coatings. EPD can be applied for a wide range of fine powder or colloidal particles of metals, ceramics, polymers, and the composites. Particularly, this method has been used widely for depositing ceramic particles on metal and alloy implant materials. The advantages of the EPD process are the short formation time, simple apparatus, and the ability to produce uniform coatings on complex geometries. Furthermore, EPD offers easy control over film thickness and morphology by simply adjusting depositing time and applied potential [22].

In this research, manufacturing nano-hardystonite and its coating on titanium substrate through electrophoretic method were carried out and the corrosion behavior, bioactivity, and biocompatibility of the synthesized bioceramics were studied.

2 Materials and methods

The hardystonite ($Ca_2ZnSi_2O_7$) bio-ceramics nanoparticles were made using sol–gel technique. Tetrahydrate calcium nitrate ($Ca(NO_3)_2{\bullet}4H_2O$, Merck, Germany), hexahydrate zinc nitrate ($Zn(NO_3)_2{\bullet}6H_2O$, Merck, Germany), nitric acid (HNO_3, Merck, Germany(, tetraethyl orthosilicate (TEOS $(C_2H_5O)_4Si$, Sigma-Aldrich, St. Louis, MO, USA) and double-distilled water (H_2O) were used as the components in this method. To prepare the hardystonite nanoparticles, the tetraethyl orthosilicate (TEOS) was mixed with 2 M nitric acid and double-distilled water (mol ratio: TEOS/H_2O/HNO_3 = 1:8:0.16) and was stirred by the magnetic stirrer for 30 min with a rotation speed of 100 per minute and the hydrolysis occurred. In this phase, the hydrolysis reaction led to the replacement of alkoxide groups with hydroxyl groups and the Si–O–Si bonds were created during the next agglomeration process. Calcium nitrate and zinc nitrate were subsequently added with a 7-min interval (mol ratio: TEOS/$Zn(NO_3)_2{\bullet}6H_2O$/$Ca(NO_3)_2{\bullet}4H_2O$ = 2:1.2). Then, the solution was stirred for 5 h at room temperature to complete the hydrolysis reaction and the resulted sol was dried at 60°C for 1 day and 120°C for 24 and 48 h, respectively. The resulted dry gel was ground and sieved to 250-mesh and sintered at 1200°C for 3 h. The phase structure of hardystonite was examined by X-ray diffraction (XRD) to confirm the crystalline structure.

The synthesized dry powders were front loaded into a 2 × 2 × 0.05 cm cavity of a glass slide. In order to observe the microstructure, scanning electron microscope (Model SUPRA 40 VP FE-SEM, Carl Zeiss AG, Germany) and transmission electron microscope (Philips-CM200-FEG) were used. Scanning electron microscopy (SEM) was carried out on samples coated with gold using a Seron Technology electron microscope and AIS 2100 detector. Powder samples were prepared for TEM observation by suspending in analytical grade ethanol, then examined using a Philips-CM10 TEM at an accelerating voltage of 100 kV.

The titanium alloy substrates (Ti-6Al-4V, Iran) with 3 mm × 1 cm × 2 cm sizes were used to perform hardystonite deposition. For better adhesion, the mentioned samples were prepared by surface preparation methods. The sample surfaces were prepared by 60, 100, 220,400, and 600 grit silicon carbide sandpapers, and then they were put in acetone solution for 10 min in the ultrasonic cleaner device to remove contamination. Upon completion of washing, the samples were dried by the laboratory dryer model GE 411 with the power supply of 1000 W. The coating was applied by the electrophoretic method.

In order to synthesize the hardystonite suspension for the coating, the methanol (CH3OH, Merck, purity ≥ 99.9%) was used as a solvent. 70 cc of the solvent was poured into the beaker. Then 3 g hardystonite was added to the solvent and the agitation carried out on the magnetic stirrer for 24 h at room temperature to gain desired uniformity. The obtained suspension was put in the ultrasonic stirrer for 30 min. The electrophoretic set was used to coat the titanium alloy samples (Ti-6Al-4V). During coating, the anode was kept at a distance of 1 cm from the cathode. Following these steps, in order to have a uniform coating, the time of samples coating was 3 min and the applied voltages were 30 V and 50 V [19]. The coated substrates were sintered in the sintering furnace at 800°C for 2 h to increase the adhesion of a coating to the substrate. Electrochemical Tafel test was conducted on coated samples in Ringer's solution. Ag/AgCl and platinum electrodes were used as reference and counter electrodes to complete the circuit and the test. Thermal element and thermometer were used as heating systems to adjust the temperature. Potentiostat–Galvanostat (IVIUMSTAT) set was applied to measure electrochemical by electrochemical polarization method. After obtaining anodic and cathodic polarization curves for each sample, the corrosion potential was specified. Subsequently, the corrosion current density was determined using Tafel extrapolation. Then, the average value of corrosion current density was calculated for each group of results.

Currently, two common methods have been used for testing in vitro bioactivity of bioceramics. One method is to evaluate the apatite-formation ability of the bioceramics in the simulated body fluid (SBF) (Noandishan co. product, Iran). The other method is to investigate in vitro bone cell response to bioceramics [18]. In this work, in order to test the in vitro biomineralization ability, the simulated body fluid (SBF) was used to study the ability of bio-ceramic hardystonite in the formation of apatite. The samples were prepared, before immersion in simulated body fluid. The area was considered 1 cm^2 for each sample. In order not to be in touch with simulated body fluid, the remainder of the samples was completely covered with lac varnish and the effective area was determined to affect the test. The coated substrates were placed in each dish and then a certain volume of simulated body fluid was added. The coating surface area/solution volume of SBF was calculated using the equation, $V_s = S_a/10$, where V_s is the volume of SBF (ml) and S_a the apparent surface area of samples (mm^2). Therefore, 10 ml of simulated body fluid was added to each container. After blocking the lid with a plastic lid, dishes were entered in a warm bath with a constant temperature of 37 ± 0.1 °C. All samples were removed from the solution after 7, 14, 21 days, rinsed with double-distilled water and dried at ambient temperature for 24 h, respectively. Scanning electron microscope (Hitachi S4160, Cold Field Emission) was used to confirm the formation of the apatite on the surface of the soaked samples and study its surface morphology.

The MTT assay (DNAbiotech Co., Iran) was used to examine the degree of hardystonite nanoparticles' toxicity. At first, the hardystonite nanoparticles were sterilized using the autoclave. 1000 cells (human bone marrow mesenchymal stem cells) were cultured in 24-well plates in standard conditions in the incubator. Then, 5, 50, 100, and 200 µg/ml (microgram per milliliter) of hardystonite powder were prepared in DMEM (Merck, Germany). The particles were placed in a 15-ml tube containing DMEM. The dispersion of particles was performed using ultra-sonic irradiation for 20 min. The culture medium of cells was changed every other day. The stem cells with a primary density of 5×10^3 were cultured in each well in the 24-well plate in DMEM containing cultured particles. After 24, 72, and 96 h of culturing, the stem cells viability was assessed by the MTT test. In each time interval, 50 microliters of MTT solution (5000 micrograms per milliliter in DMEM) was added to each well. After passing each time, the surface layer of each well was evacuated and in order to dissolve the formazan crystals, 200 µl dimethyl sulfoxide was added to each well and they were put in a dark room for 2 h at room temperature. Optical density at a wavelength of 570 nm was read by the spectrometry method. A similar process was considered for stem cells without hardystonite nanoparticles as control samples. All measurements were conducted at least three samples ($n = 3$), and all results were presented as mean and standard deviation. Moreover, the one-way analysis of variance (ANOVA) was applied to compare the results. The amount of (p value) less than 0.05 was significant statistically.

3 Results and discussion

Figure 1 shows the evaluation results of hardystonite phase structure by X-ray diffraction (XRD) test. In this figure, it is obvious that only hardystonite phase peaks are available, suggesting the creation of pure and completely crystalline hardystonite phase. The highest peak for hardystonite is located at $2\theta = 31°$ of calcined powder at 1200 °C. According to [7], calcination temperature is critical to the purity of the prepared powders and when temperature increased to 1200 °C, pure hardystonite powders were obtained. The hardystonite powder elemental analysis is shown in Table 1 and Fig. 2. These findings indicated that the three main elements in hardystonite bio-ceramic are zinc (Zn), silicon (Si), and calcium (Ca) with defined degrees in the final composition.

Figure 1 shows the evaluation results of hardystonite phase structure by X-ray diffraction (XRD) test. In this figure, it is obvious that hardystonite phase is dominant phase in the structure. The highest peak for hardystonite is

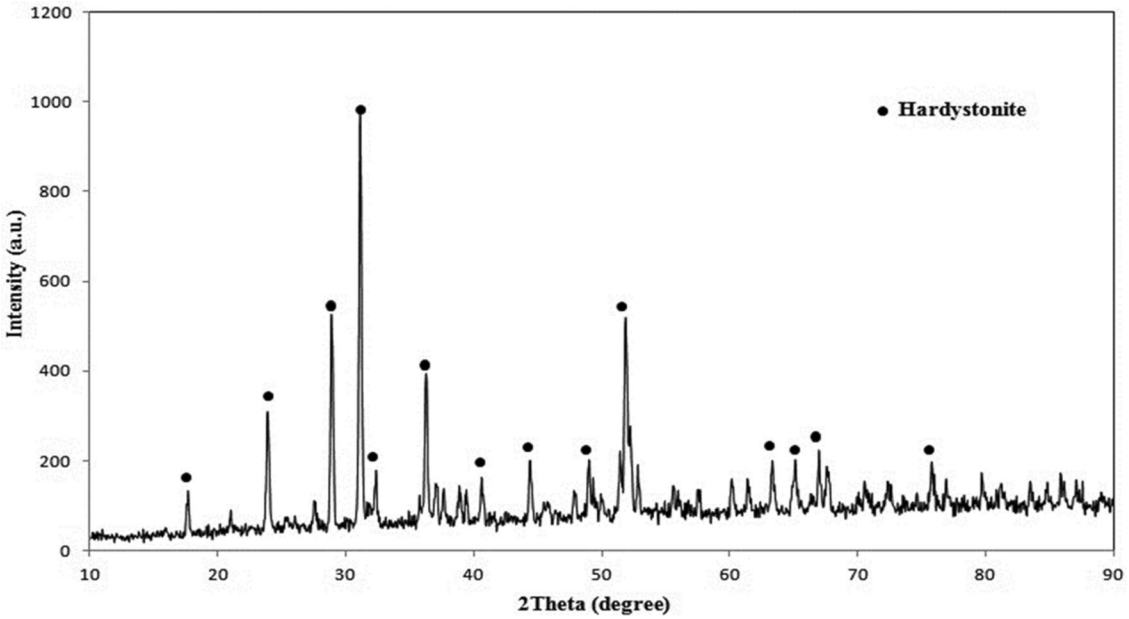

Fig. 1 X-ray diffraction pattern of hardystonite bio-ceramic calcined at 1200 °C

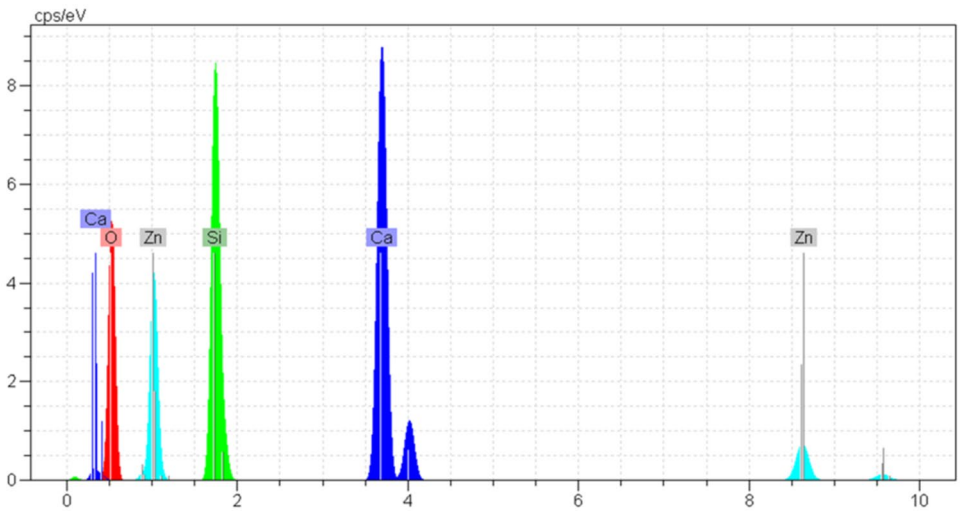

Fig. 2 Energy-dispersive X-ray analysis (EDX) of hardystonite nano-powder

located at $2\theta = 31°$ of calcined powder at 1200 °C. According to [7], calcination temperature is critical to the purity of the prepared powders and when temperature increased to 1200 °C, pure hardystonite powders were obtained. However, our results are in consistent with Bagherpor et al. [19] findings, once trace of carbon element originated from initial material could be find in the EDX analysis (Table 1) and those non-attributed peaks in the XRD analysis can be assign to the carbon-based contaminants. The hardystonite powder elemental analysis is shown in Table 2 and Fig. 2. These findings indicated that the three main elements in hardystonite bio-ceramic are zinc (Zn), silicon (Si), and calcium (Ca) with defined degrees in the final composition.

Table 2 Weight percentage of hardystonite constituents measured using energy-dispersive X-ray analysis (EDS)

Element	Concentration (Wt%)
C	6.7
Si	14.2
Zn	16.5
Ca	17.9
O	46.2

Scanning electron microscope (SEM) images (Fig. 3) show the morphology and the sizes of hardystonite ceramics particles. It shows that the nanoparticles in very small sizes (< 70 nm in diameter) or big agglomerates were formed and

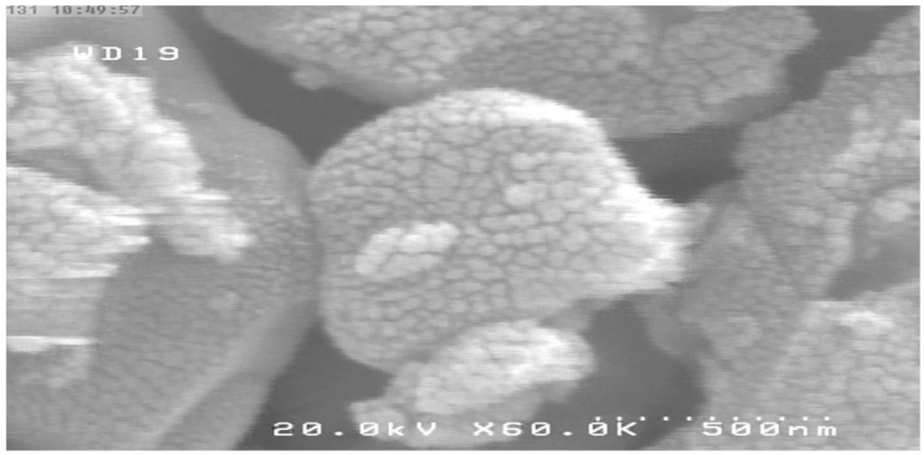

(a)

Fig. 3 Scanning electron microscope (SEM) images of hardystonite particles

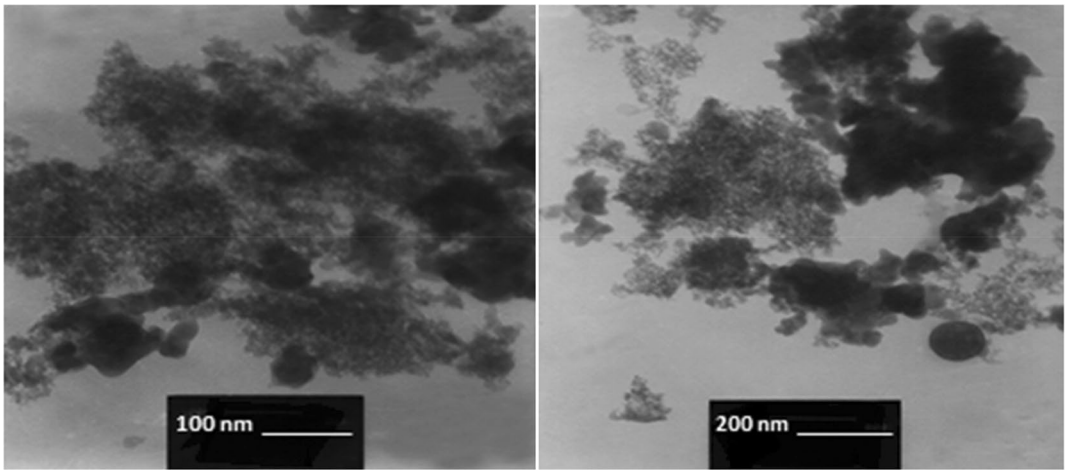

Fig. 4 TEM micrograph of produced hardystonite powder particles calcined at 1200 °C for 3 h

are in conformity with the previous studies [23]. This SEM micrograph shows that the grain size of hardystonite ceramic was smaller than 5 µm. Reaching this morphology and size for the hardystonite particles is due to the use of sol–gel technique and corresponds to the findings of other researchers [7]. The size and morphology of bio-ceramics particles obtained by sol–gel process are effective in the formation of homogeneous and uniform coating [24]. Figure 4 shows survey results of the morphology of produced particles by transmission electron microscope (TEM). The nanometer size of the particles and the rounded shape of crystallite are well seen in this figure. The morphology and boundary size of particles (less than 100 nm) match with previous studies [7].

Production of hardystonite nanoparticles regardless of their advantages in formation of the homogeneous coating also plays a very important role in other aspects [7]. In many cases, dissolving the ceramic powder in other solutions such as silica sol for coating is performed by sol–gel method [20].

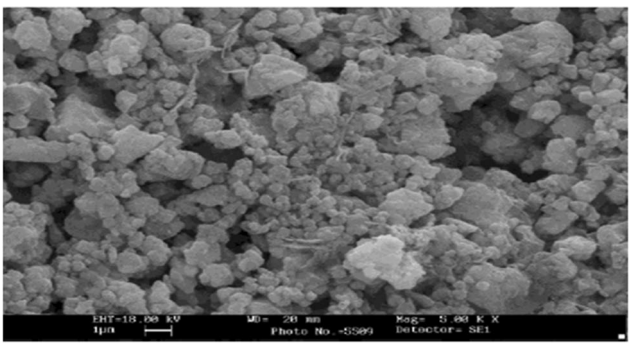

Fig. 5 Coated samples after immersion in simulated body fluid (SBF), after 7 days

Some researchers applied this technique for bioactive glass coating on a metal substrate [20, 25–27]. As can be seen in Fig. 5, the hardystonite coating applied by electrophoretic has a uniform structure with no cracks. It can be concluded

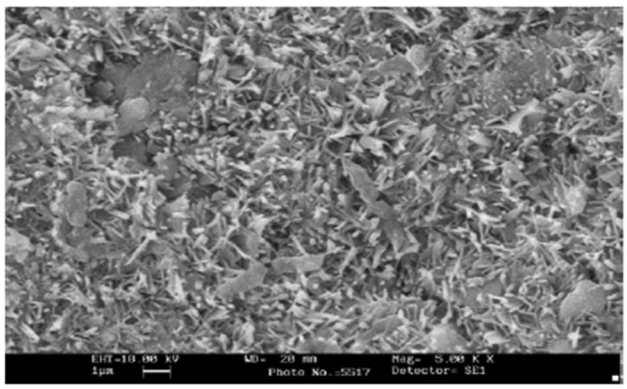

Fig. 6 Coated samples after immersion in simulated body fluid (SBF), after 14 days

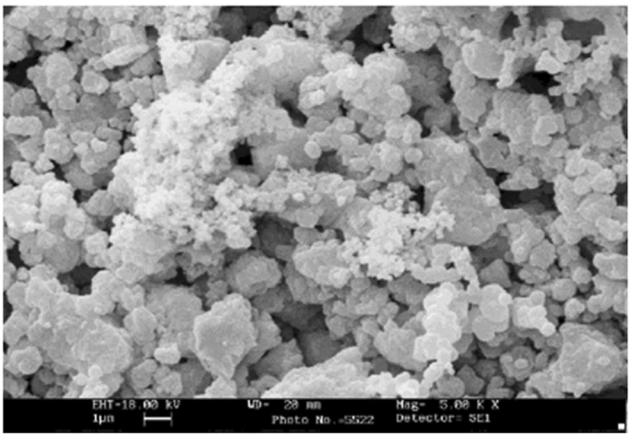

Fig. 7 Coated samples after immersion in simulated body fluid (SBF), after 21 days

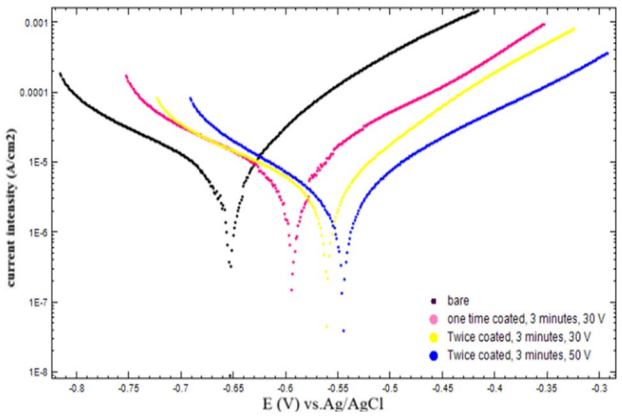

Fig. 8 Tafel polarization diagram of titanium samples (Ti-6Al-4V) with and without coating in Ringer's solution

Table 3 The average corrosion potential and current density of the bare and coated samples

Test specimens	E. Corr (mV)	I Corr (μA/cm^2)
Substrate	− 660	1.92
Once-coated sample, 30 V, 3 min	− 591	2.14
Twice-coated sample, 30 V, 3 min	− 562	1.61
Twice-coated sample, 50 V, 3 min	− 542	1.04

that the electrophoretic technique can result in a homogenous structure with no crack on metal substrates. This result is in agreement with the results of other studies [28, 29]. A homogenous and uniform coating with no external defects is the most important purpose of the coating by the electrophoretic technique. Such a coating is essential to achieve appropriate corrosion and suitable biological properties for the substrates [30].

Figures 5, 6, and 7 demonstrate the images of coated samples after immersion in simulated body fluid (SBF). The ion concentrations of the SBF are similar to those of human body plasma [28]. As can be seen, the first sample was immersed for 7 days in simulated body fluid (SBF) and no specific changes are seen in morphology in comparison with the images of coating before putting in simulated body fluid (SBF). Apparently no apatite has also been formed on the coating. It is clear that a needle-shaped compound has germinated in the second sample within 14 days in simulated body fluid (SBF). It can be concluded from the SEM images that the needle-shaped compound can be completely formed by changing days from 14 to 21 days. In this way, an apatite structure becomes similar to the desirable structure of Cauliflower-like [6]. Using simulated body fluid (SBF) is an efficient method to evaluate bioactivity and determine the formation of apatite and quasi-apatite structures on the ceramic surface. Therefore, the formed compositions on a substrate after immersion in SBF are most probably a calcium phosphate-based composition [29, 31]. What can we conclude from SEM images and according to the morphology of the participated layers is formation of a calcium phosphate-based material [19]. Structural analysis methods such as XRD or FTIR are required to determine what compositions have been exactly formed on the hardystonite surface.

Figure 8 shows the Tafel polarization diagram of titanium samples (Ti-6Al-4V) both with coating and without hardystonite coating in Ringer's solution. Table 3 shows the average of corrosion density and corrosion potential of titanium substrate without and with coating in Ringer's solution specified by polarization diagrams and Tafel extrapolation method. According to Table 3 and Fig. 8, titanium (Ti-6Al-4V) without coating shows more corrosion density in normal Ringer's solution (I_{corr} = 1.92 μA/cm^2). The corrosion density of twice coated titanium (Ti-6Al-4V) with voltage 50 in normal Ringer's solution decreased (I_{corr} = 1.04 μA/cm^2). By comparing the diagrams, it was observed that by applying

hardystonite coating, potential tends to have more positive values and corrosion current density decreases, indicating further protection against corrosion compared to bare titanium alloy. The potential value of coated samples (sample 4), (− 542 mV vs. Ag/AgCl) increased in comparison with non-coated samples (− 660 mV vs. Ag/AgCl). According to Fig. 8 and Table 3, the current density of once-coated samples with voltage 30 (sample 2) increased compared to the non-coated substrate (sample 1). The reason for the increase is the formation of porous coatings with high pores, which cause pitting and local corrosion of the underlying substrate [32–34]. The corrosion current density of the twice-coated sample with voltage 30 (sample 3) decreased in comparison with that of non-coated sample. In fact, the coating has been successful in improving corrosion behavior in the substrate. The reason for this decrease is the reduction in porosity and pores in the twice-coated substrate. The corrosion current density of the twice-coated sample with 50 V decreased in comparison with other samples and this coating was performed better than two previous coatings. Due to the increase in coating voltage, the amount of ceramic deposited on the substrate increases, and consequently, the coating thickness develops. It can be concluded that the resistance to substrate corrosion increases by increasing the voltage to 50 V and frequency of coating.

3.1 Assessment of the results of cytotoxicity

Figure 9 clarifies the MTT measurement results of hardystonite particles. As it is shown in this figure, on the first and second days of the culture, no significant differences were observed in the viability and proliferation of stem cells exposed to hardystonite nanoparticles in different concentrations ($p > 0.05$). After 3 days, the cells with 50 micrograms per milliliter concentration showed better vitality and reproduction compared to the control sample ($p < 0.05$). After 5 days, only the cells, which were exposed to 50 mg particles, showed higher viability in comparison with other groups (Fig. 9).

Therefore, it is inferred that the optimized density to evaluate the cell culture for such samples is 50 mg/ml and the appropriate time is after 5 days of culture. The findings revealed that hardystonite increases the vitality and reproduction of stem cells [31]. It is believed that zinc ions released from the ceramics play a very important role in stimulating the reproduction of cells [35]. Reffitt et al. [36] reported that the density of released silicon ions from the silicon-based ceramics containing zinc like hardystonite amounts to the physiologic density (0.005–0.02 micromolar) of this ion in plasma. It is also reported that the orthosilicate acid in physiologic densities stimulates the collagen type I cells similar to osteoblast cells and helps to the differentiation of osteoblast cells [8]. In many studies, the bioactive glasses and silicon bio-ceramics are suggested to be a stimulating factor for osteoblasts [8]. Calcium (Ca) which is found in hardystonite is also another main factor in composing and metabolism of bone [27]. The relatively high bioactivity of hardystonite is due to calcium ion in its composition. The results obtained in this study allow us to conclude that hardystonite as a bioactive ceramic possesses a great biological potential, and further investigation should be done to promote commercialization and encourage its use in hard tissue engineering and bone repair.

4 Conclusion

1. Hardystonite nanoparticles ($Ca_2ZnSi_2O_7$) synthesis was obtained by the sol–gel technique.
2. Electrophoretic deposition method was utilized in order to apply the hardystonite nanoparticles on titanium alloy substrate (Ti-6Al-4V).
3. The calcination temperature and time for hardystonite application on the substrate were set at 800 °C and 2 h,

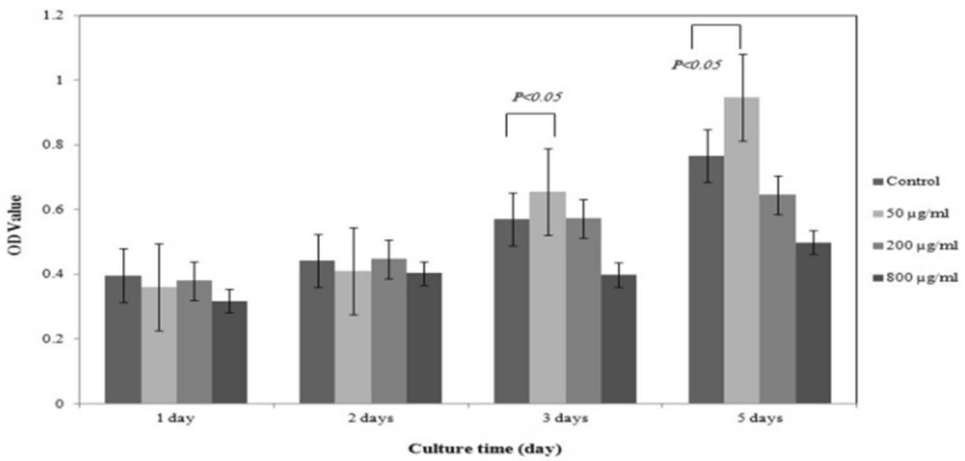

Fig. 9 MTT measurement results of hardystonite particles

respectively, in order to achieve the best adhesion quality.
4. Increase the voltage and the time of coating create a more homogenous layer on the titanium substrate.
5. The bioactivity of produced hardystonite on the surface is acceptable; hydroxyapatite was made on the substrate, after 21 days of immersion in simulated body fluid (SBF).
6. The hardystonite coating has a desirable effect on corrosion resistance of the titanium alloy substrate and reduces the corrosion density of the substrate. This implies that the implant corrosion resistance increases and subsequently the release of metal ions and their destructive effects on human body tissues decrease. The titanium alloy coated with hardystonite has higher corrosion resistance in comparison with the substrate without coating.
7. Non-toxicity of the hardystonite nanoparticles exposed to osteoblast stem cells was confirmed and it was observed that cell reproduction increases at low concentrations.

Acknowledgements The authors' deep appreciation is extended to Shahrekord University for superb technical assistance.

References

1. R. Emadi, S. Sadeghzade, F. Tavangarian, Evaluation of bioactivity and mechanical properties of silica-based ceramic for using in tissue engineering application. Materials Science and Technology 2019, MS and T 2019- Portland, United States, 1302–1309 (2019)
2. L.L. Hench, Bioceramics. J. Am. Ceram. Soc. **81**(7), 1705–1728 (1998)
3. W. Xiaopeng, K. Fantao, H. Biqing, C. Yuyong, Electrochemical corrosion and bioactivity of Ti-Nb-Sn-hydroxyapatite composites fabricated by pulse current activated sintering. J. Mech. Behav. Biomed. Mater. **75**, 222–227 (2017)
4. L.L. Hench, J. Wilson, An introduction to bioceramics. World Sci. **1**, 114–129 (1993)
5. M. Jarcho, Calcium phosphate ceramics as hard tissue prosthetics. Clin. Orthop. Relat. Res. **57**, 259–278 (1981)
6. H.A. El-Hamid, S.M. Abo-Naf, R.L. Elwan, Characterization, bioactivity investigation and cytotoxicity of borosilicate glass/dicalcium silicate composites. J. Non-Cryst. Solids **512**, 25–32 (2019)
7. C. Wu, J. Chang, W. Zhai, A novel hardystonite bioceramic: preparation and characteristics. Ceram. Int. **31**(1), 27–31 (2005)
8. C. Pontremoli, I. Izquierdo-Barba, G. Montalbano, M. Vallet-Regí, C. Vitale-Brovarone, S. Fiorilli, Strontium-releasing mesoporous bioactive glasses with anti-adhesive zwitterionic surface as advanced biomaterials for bone tissue regeneration. J. Colloid Interface Sci. **563**, 92–103 (2020)
9. G. Parande, V. Manakari, S. Prasadh, D. Chauhan, S. Rahate, R. Wong, M. Gupta, Strength retention, corrosion control and biocompatibility of Mg–Zn–Si/HA nanocomposites. J. Mech. Behav. Biomed. Mater. **103**, 103584 (2020)
10. F.L. Nie, Y.F. Zheng, S.C. Wei, C. Hu, G. Yang, In vitro corrosion, cytotoxicity and hemocompatibility of bulk nanocrystalline pure iron. Biomed. Mater. **5**(6), 65015 (2010)
11. C.-C. Shih, S.-J. Lin, Y.-L. Chen, Y.-Y. Su, S.-T. Lai, G.J. Wu, C.-F. Kwok, K.-H. Chung, The cytotoxicity of corrosion products of nitinol stent wire on cultured smooth muscle cells. J. Biomed. Mater. Res. **52**, 395–403 (2000)
12. Erasmus, E. P. I., "Synthesis, testing and characterization of porous biocompatible porous bioactive glasses for clinical use." PhD diss., 2017
13. S.F.S. Shirazi et al., A review on powder-based additive manufacturing for tissue engineering: selective laser sintering and inkjet 3D printing. Sci. Technol. Adv. Mater. **16**(3), 033502 (2015)
14. M. Kaur, K. Singh, Review on titanium and titanium based alloys as biomaterials for orthopaedic applications. Mater. Sci. Eng. C **102**, 844–862 (2019)
15. S. Raynaud, E. Champion, D. Bernache-Assollant, P. Thomas, Calcium phosphate apatites with variable Ca/P atomic ratio I. Synthesis, characterisation and thermal stability of powders. Biomaterials **23**(4), 1065–1072 (2002)
16. P. Bhattacharya, S. Neogi, *Techniques for deposition of coatings with enhanced adhesion to bio-implants* (Scrivener Publishing, Salem, 2017), pp. 235–256
17. M. Ganjali, A. Yazdanpanah, M. Mozafari, Laser deposition of nano coatings on biomedical implants. Emerg. Appl. Nanoparticles Arch. Nanostruct., 235–254 (2018)
18. H. Gheysari, E. Karamian, Prepration and characterization of hydroxyapatite reinforced with hardystonite as a novel bio-nanocomposite for tissue engineering. NBM **2**(1), 141–152 (2015)
19. I. Bagherpour, S.M. Naghib, A.H. Yaghtin, Synthesis and characterization of nanostructured hardystonite coating on stainless steel for biomedical application. IET Nanobiotechnol. **12**(7), 895–902 (2018)
20. A. Santos-Coquillat, M. Mohedano, E. Martinez-Campos, R. Arrabal, A. Pardo, E. Matykina, Bioactive multi-elemental PEO-coatings on titanium for dental implant applications. Mater. Sci. Eng. C **97**, 738–752 (2019)
21. P. Srinath, P. Abdul Azeem, K. Venugopal Reddy, Review on calcium silicate-based bioceramics in bone tissue engineering. Int. J. Appl. Ceram. Technol. **17**(5), 2450–2464 (2020)
22. K.E. Fox, N.L. Tran, T.A. Nguyen, T.T. Nguyen, P.A. Tran, Surface modification of medical devices at nanoscale-recent development and translational perspective. Bomater. Transl. Med., 163–189 (2019)
23. A. Doostmohammadi, A. Monshi, R. Salehi, M.H. Fathi, Z. Golniya, A.U. Daniels, Bioactive glass nanoparticles with negative zeta potential. Ceram. Int. **37**(7), 2311–2316 (2011)
24. C. Garcia, S. Cere, A. Duran, Bioactive coatings prepared by sol–gel on stainless steel 316L. J. Non. Cryst. Solids **348**, 218–224 (2004)
25. H. Mohammadi, M. Hafezi, S. Hesaraki, M.M. Sepantafar, Preparation and characterization of Sr-Ti-hardystonite (Sr-Ti-HT) nanocomposite for bone repair application. Mashhad Univ. Med. Sci. **2**(3), 203–210 (2015)
26. C. Wu, Y. Ramaswamy, J. Chang, J. Woods, Y. Chen, H. Zreiqat, The effect of Zn contents on phase composition, chemical stability and cellular bioactivity in Zn-Ca-Si system ceramics. J. Biomed. Mater. Res. Part B Appl. Biomater. **87B**(2), 346–353 (2008)
27. B. Wegener, B. Sievers, S. Utzschneider et al., Microstructure, cytotoxicity and corrosion of powder-metallurgical iron alloys for biodegradable bone replacement materials. Mater. Sci. Eng. B **176**(20), 1789–1796 (2011)
28. W. Zhao, J. Wang, W. Zhai, Z. Wang, J. Chang, The self-setting properties and in vitro bioactivity of tricalcium silicate. Biomaterials **26**(31), 6113–6121 (2005)

29. H. Ohgushi, A.I. Caplan, Stem cell technology and bioceramics: from cell to gene engineering. J. Biomed. Mater. Res. **48**(6), 913–927 (1999)
30. B. Zhang, C.T. Kwok, F.T. Cheng, H.C. Man, Fabrication of nano-structured HA/CNT coatings on Ti6Al4V by electrophoretic deposition for biomedical applications. J. Nanosci. Nanotechnol. **11**(12), 10740–10745 (2011)
31. H. Gheisari, E. Karimian, M. Abdellahi, A novel hydroxyapatite–Hardystonite nanocomposite ceramic. Ceram. Int. **41**(4), 5967–5975 (2015)
32. L. Li, J. Gao, Y. Wang, Evaluation of cyto-toxicity and corrosion behavior of alkali-heat-treated magnesium in simulated body fluid. Surf. Coat. Technol. **185**(1), 92–98 (2004)
33. A.K. Jaiswal, H. Chhabra, S.S. Kadam, K. Londhe, V.P. Soni, J.R. Bellare, Hardystonite improves biocompatibility and strength of electrospun polycaprolactone nanofibers over hydroxyapatite: a comparative study. Mater. Sci. Eng. C **33**(5), 2926–2936 (2013)
34. X. Zhang, Y. Wu, Y. Xue, Z. Wang, L. Yang, Biocorrosion behavior and cytotoxicity of a Mg–Gd–Zn–Zr alloy with long period stacking ordered structure. Mater. Lett. **86**, 42–45 (2012)
35. M. Zhang, W. Zhai, J. Chang, Prepration and characterization of a novel willemite bioceramic. Mater. Sci. **21**, 1169–1173 (2010)
36. D.M. Reffitt, J. Meenan, J.D. Sanderson, R. Jugdaohsingh, J.J. Powell, R.P. Thompson, Bone density improves with disease remission in patients with inflammatory bowel disease. Eur. J. Gastroenterol. Hepatol. **15**(88), 1267–1273 (2003)

Publisher's Note Springer Nature remains neutral with regard to jurisdictional claims in published maps and institutional affiliations.